Absolute frequencies of the ^{6,7}Li $2S\ ^2S_{1/2} \rightarrow 3S\ ^2S_{1/2}$ transitions

Yu-Hung Lien,[1,*] Kuan-Ju Lo,[1] Hsuan-Chen Chen,[2] Jun-Ren Chen,[1] Jyun-Yu Tian,[2] Jow-Tsong Shy,[1,2] and Yi-Wei Liu[1,†]

[1]*Department of Physics, National Tsing Hua University, Hsinchu 30013, Taiwan*

[2]*Institute of Photonics Technologies, National Tsing Hua University, Hsinchu 30013, Taiwan*

(Received 20 October 2010; published 31 October 2011)

The measurement of the absolute frequencies of the $2S \rightarrow 3S$ of atomic lithium is reported. To reduce systematic effects, we employed a frequency-comb-stabilized excitation laser, a weakly collimated atomic beam, and the cascading $2P \rightarrow 2S$ 670 nm fluorescence as the signal. The transition frequencies, including two isotopes (^{6,7}Li), were measured to an accuracy of $<$ 330 kHz. In comparison with the previous GSI Group experiment, the frequency of the $2S_{1/2} \rightarrow 3S_{1/2}$ transition of ^{7}Li is 815 618 181.45(9) MHz, which is improved by a factor of 2. The resultant hyperfine constants of the $3S$ state and the deduced difference of the nuclear charge radii $\delta\langle r_c^2\rangle$ from the isotope shift are in good agreement with previous results. Since a more straightforward methodology is adopted, our measurement is less model dependent and serves as an independent investigation of the reported transitions.

DOI: 10.1103/PhysRevA.84.042511 PACS number(s): 32.30.−r, 32.80.Wr, 42.62.Fi

I. INTRODUCTION

High precision spectroscopy of simple atomic systems has been crucial in diverse fields of physics, such as the determination of fundamental constants [1,2] and exotic nuclear structure [3,4]. Many of these studies demand high precision calculations [5,6] involving high-order relativistic and QED corrections. Adequate tools, like absolute transition frequency measurement, become critical to benchmark the developed theoretical works. The study of the lithium atom poses a great challenge because of the four-body coulombic nature obscuring the calculation of the high-order corrections. The absolute frequency measurement of the Li $2S \rightarrow 3S$ transition can offer very high precision data to benefit the relevant studies.

The energy of atomic lithium can be expressed as the nonrelativistic energy, the relativistic correction, the QED correction, and the finite nuclear size correction. The most accurate treatments solve the nonrelativistic Schrödinger equation variationally in multiple-basis sets in Hylleraas coordinates [7–9] and use the resultant wave functions to calculate relativistic and QED corrections perturbatively. Recent calculations of $2S \rightarrow 2P, 2S \rightarrow 3S$ transition energies and their mass-dependent isotope shifts (IS) reported a relative accuracy of better than 1×10^{-7} [7,10], and the calculation accuracy of the hyperfine splitting was better than 1×10^{-4} [11]. The partial energy diagram of atomic lithium is shown in Fig. 1.

The recent progress in experimental work mostly concentrates on the low-lying states. The work of the $2S \rightarrow 2P$ transition has been reported by Refs. [12–15] and the $2S \rightarrow 4S$ transition by Ref. [16]. Owing to the high interest in the neutron-rich nucleus, the GSI Group finished a series of works on the $2S \rightarrow 3S$ transition of Li isotopes [4,17–21]. They performed the two-photon spectroscopy by a cavity-enhanced laser radiation and an atomic beam. The spectroscopic signal was detected using the complicated multistage resonance photoionization because of the limited amount of the heavier isotopes, such as ^{8,9,11}Li. This scheme was also applied to the absolute frequency measurement of ^{6,7}Li [17,18]. However, the asymmetry of the line shapes caused by the strong ac Stark effect was the dominant systematic effect and required sophisticated line shape analysis. Instead of the aforementioned complex detection, we detected the signal via the 670 nm $2P \rightarrow 2S$ cascade fluorescence and used only a weaker excitation laser without the ionization laser to diminish the systematic effect. Therefore, a weaker ac Stark effect and symmetrical line shape were obtained and led to an uncertainty $<$330 kHz.

II. EXPERIMENT

The apparatus is shown in Fig. 2. A single frequency Ti:sapphire laser was pumped by an 8-W 532-nm solid state laser and generated 1-W 735-nm radiation. The laser beam was then split into four parts for spectroscopy, frequency control, wavelength measurement, and diagnosis. The beam for the lithium spectrometer was modulated using an optical chopper with a 690-Hz 50% duty cycle square wave. It was then focused to a spot size of 100 μm in a weakly collimated atomic beam using focal length, $f = 250$-mm lens and retroreflected by a concave mirror with radius of curvature, $R = 500$ mm. The laser frequency was simultaneously monitored using a Fabry-Pérot reference cavity and a wavelength meter. Before entering the atomic beam chamber, a 6.5-m-long optical path was implemented using several high reflection mirrors to reduce the frequency shift induced by the noncollinearity of two counterpropagating beams, i.e., the first-order Doppler shift. One part of the beams was sent to the optical frequency comb (OFC) via an optical fiber for frequency control. The self-referenced optical frequency comb was based on a 1-GHz mode-locked Ti:sapphire laser whose spectrum was expanded using a microstructure fiber. To ensure the long term frequency accuracy and stability, all of the rf sources for our OFC and frequency measuring instruments were referenced to a global positioning system (GPS)-disciplined Rb oscillator.

*Present address: Dipartimento di Fisica, Universita' di Firenze, Sesto Fiorentino, Italy.

†ywliu@phys.nthu.edu.tw

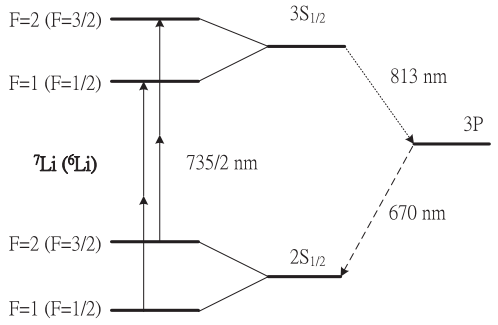

FIG. 1. Partial level diagram of atomic lithium (not to scale).

The details of the OFC setup can be found in [22]. The precise frequency control of the Ti:sapphire laser was realized by locking the beat frequency between the Ti:sapphire laser and the OFC to a frequency synthesizer via a phase-locked loop. The frequency of the Ti:sapphire laser was then able to be scanned stepwise by tuning the computer-controlled synthesizer frequency. Such a scheme allows us to have both precise laser frequency control and a long integration time to suppress the noise. The range of the continual frequency scanning was limited to 350 MHz due to the OFC repetition frequency. Nevertheless, the scanning range was large enough to cover the region of interest in the spectrum of each transition.

The weakly collimated atomic beam was generated from a stainless steel oven which was wrapped by a resistive heating wire. The temperature of the oven was maintained at $570 \pm 1\,^{\circ}$C, and the corresponding vapor pressure was estimated to be 3.1 Pa within the oven. The atomic beam divergence defined by a 5-mm oven opening and a 10-mm aperture 67-mm away from the oven is 220 mrad. The laser beam was focused at 1-cm away from the aperture. The lithium strip is 99.99% in purity and its abundance is natural. The fluorescence signal was collected using an 1-in. lens of $f = 25$ mm and then detected by a photomultiplier (PMT). In order to block the stray light, a filter assembly combining a 670-nm 3-nm full width at half maximum (FWHM) laser line filter and a short pass filter to further block scattered light at 735 nm were placed in front of the PMT. The signal from the PMT was demodulated by a lock-in amplifier with 30-Hz-noise bandwidth.

In the stepwise scanning, both the fluorescence signal and the beat frequency were synchronously measured with a gate time of 0.1 s. In each frequency step, five data points were averaged, and the effective integration time was then 0.5 s. Because of the limited continual scanning range, only the spectra of two ^{6}Li hyperfine transitions can be acquired in a single 180-MHz-frequency scan with a 500-kHz increment. The two hyperfine transitions of ^{7}Li were individually recorded in 40-MHz frequency scans with a 300-kHz increment. The larger increment for ^{6}Li was chosen to shorten the scan time which was limited by the duration of the Ti:sapphire laser staying locked to the OFC. The spectra of ^{6,7}Li $2S \rightarrow 3S$ hyperfine transitions are shown in Fig. 3. The signal-to-noise ratios of ^{7}Li and ^{6}Li transitions are $\sim$210 and $\sim$80, respectively. The frequency center of the transitions was determined by binning the data with 100-kHz bins and then fitting them with a spectral line shape of the Voigt-function model. The 100-kHz bin size, which is about the size of the beat frequency distribution (see Fig. 6) and meets the criterion suggested by the "Scott rule" [23], was chosen to avoid a possible binning shift. There is no improvement and difference found using a smaller bin size.

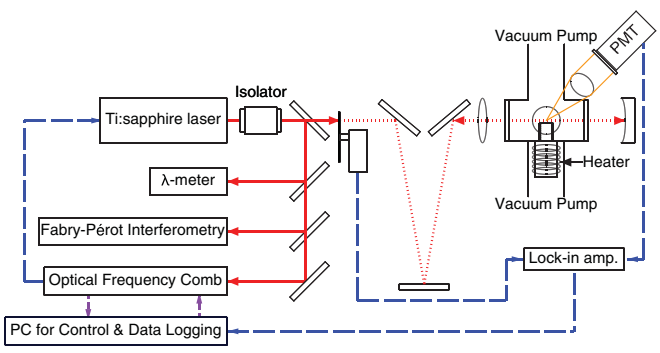

FIG. 2. (Color online) Experimental apparatus.

The Voigt function was used to incorporate several broadening mechanisms in experimental line shape fitting. The line shape asymmetry caused by a strong ac Stark shift ($\sim$4 MHz) coupled with the inhomogeneity of distributions of the laser intensity was reported as the major source of the systematic errors in the previous experiment [18]. Nevertheless, it is negligible in our experiment because the experimental ac Stark shift $<$400 kHz is much less than the natural linewidth. The random fluctuation of the fitting residual in Fig. 3 demonstrates the symmetric appearance. Therefore, there is no sophisticated model required and such a systematic effect is mostly eliminated. The upper level lifetime contributes $\sim$5.4 MHz [24] to the Lorentzian width. Due to the large divergence and the high velocity of the atomic beam, the width of the Gaussian background was estimated to be 1 GHz, which was much larger than the natural linewidth. According to the area rule of two-photon transition [25], the contribution of the Doppler background was negligible in our experiment. The transit time broadening was estimated to be 6 MHz by the 100-μm-spot size and the 1500 m/s atomic mean velocity. Meanwhile, because the optical intensity was far below the saturation intensity, the power broadening was negligible. The experimental results show the FWHM to be 8 to 10 MHz in laser frequency. Aside from the contribution from the lifetime and the transit time broadening, the residual Gaussian part of the linewidth is mainly from the fast laser jitter in a time scale of less than a millisecond, which was observed in the beat note signal using a spectrum analyzer and can be obtained from extrapolation of Fig. 6.

The uncertainties of the center frequencies of individual measurements are from 80 to 300 kHz for various measurement conditions and are shown as error bars in Fig. 4. The dominant limiting factor of the uncertainty in a single measurement is the signal-to-noise (S/N) ratio of the signal. The possible sources of the noise include: the background scattering, electronic noise, and so forth. However, the excess noise of the signal caused by laser frequency instability ultimately limits the S/N ratio, e.g., frequency modulation (noise) transferred to signal modulation (noise) by the response curve (the spectrum profile). In our experiment, only the ^{7}Li ($F = 2$–2) transition reaches this limitation, because its signal is high enough

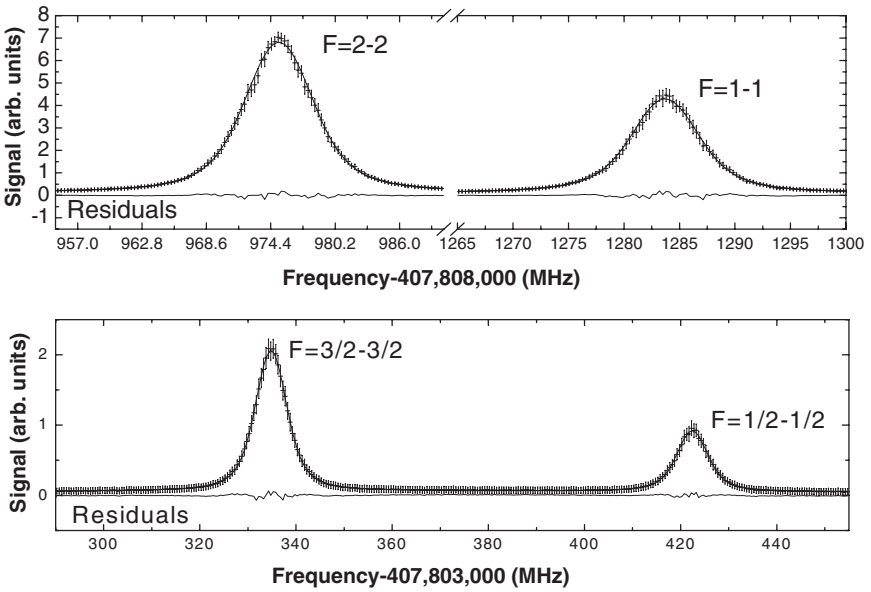

FIG. 3. Typical spectra of ^{7}Li (upper) and ^{6}Li (lower) hyperfine transitions. The horizontal axes are the laser frequency. The solid lines show the fitting residuals.

to overcome the other noise sources. All the other three transitions are still subject to the background noise, and the resulted uncertainties are larger than the 75 kHz frequency uncertainty.

All four hyperfine transitions were measured with various laser excitation powers over a period of two months. The ac Stark shifts were then corrected by a linear extrapolation as shown in Fig. 4. A linear function $\nu = \nu_0 + k\,P_{\rm laser}$ was used in the fitting to extract the transition frequency ν_0 with the least χ^2. The errors of the offset ν_0 result in the final statistical uncertainties of our measurement. The transition frequency uncertainty caused by the observed 4% laser intensity drift, the second item in the uncertainty budget table (see Table I), was estimated to be 20 kHz maximum and was small compared with the uncertainty of the fitted shift. Our results are comparable with Ref. [18] and theoretical estimates. With the ac Stark shift correction applied to all the measurements, Fig. 5, which illustrates the chronologically ordered ^{7}Li $F = 2$–2 absolute frequency measurements, shows no drift during the course of the experiment.

Besides the ac Stark shift, the residual first-order Doppler shift arising from the imperfect collinearity of the retroreflected beam significantly contributes to the systematic errors as well. The misalignment 1 mrad of retroreflection causes about 1.8-MHz blue shift to the transition frequencies. Therefore, the 6.5-m-long optical path was set up for preliminary alignment. In our experiment, we visually adjusted the counterpropagating beams to reduce the misalignment to less than 1 mm and the corresponding shift was less than 270 kHz. To further reduce this systematic error, we took advantage of the sensitivity of the signal strength to misalignment. The

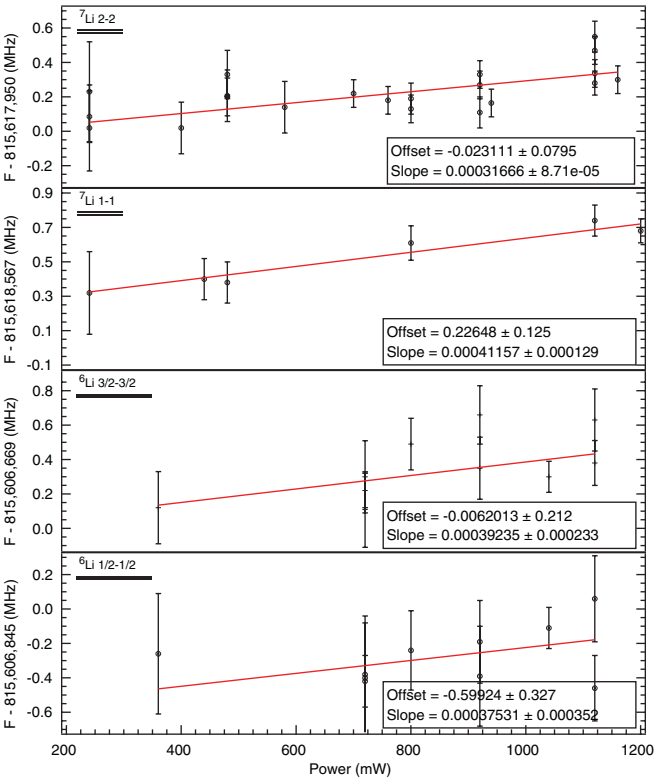

FIG. 4. (Color online) ac Stark shifts of the four transitions. The data points were fitted into a function of $\nu = \nu_0 + k\,P_{\rm laser}$. $P_{\rm laser}$ is the total radiation power in the interaction region.

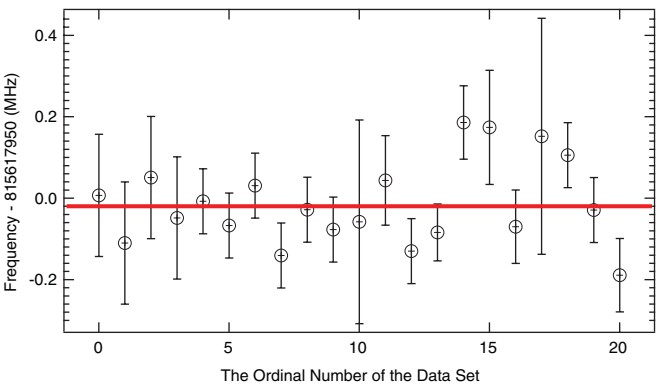

FIG. 5. (Color online) Chronological distribution of the ^{7}Li $F = 2$–2 absolute frequency measurements. The horizontal red line represents the resulting absolute frequency.

TABLE I. Uncertainty budget of the absolute frequency measurement.

Effect (source)	MHz
Statistical (zero laser power extrapolation)	0.08–0.32
ac Stark shift (laser power drift)	<0.02
First-order Doppler (beam collinearity)	0.088
Frequency comb	<0.005
Second-order Doppler (velocity of atom)	Negligible
Total	0.12–0.33

misalignment of the retroreflected beam means a smaller laser beam overlapping and therefore a smaller signal strength. A shift of 108 kHz was experimentally observed by misaligning the laser beam until the signal dropped to 50%. Before each measurement, the retroreflecting mirror was fine tuned to optimize the signal strength and, therefore, the collinearity. Practically, the variation of the signal strength was observed within 10%, and the corresponding potential shift was <88 kHz (equivalent to a 0.049-mrad misalignment) by our simulation.

The Allan deviation of the beat frequency is shown in Fig. 6, and the inset is the histogram for the beat frequency with a gate time of 0.1 s. The standard deviation of the beat frequency was determined to be 75 kHz by fitting the histogram with a single Gaussian profile. Our OFC has been checked by measuring the Comité international des poids et mesures (CIPM) recommended 532-nm I_2 $R(56)$ 32–0 a_{10} hyperfine transition, and the fractional difference is 5.3×10^{-12}. The corresponding frequency uncertainty of our OFC is <5 kHz in this measurement. The uncertainties of the measurement from various systematic effects are summarized in Table I.

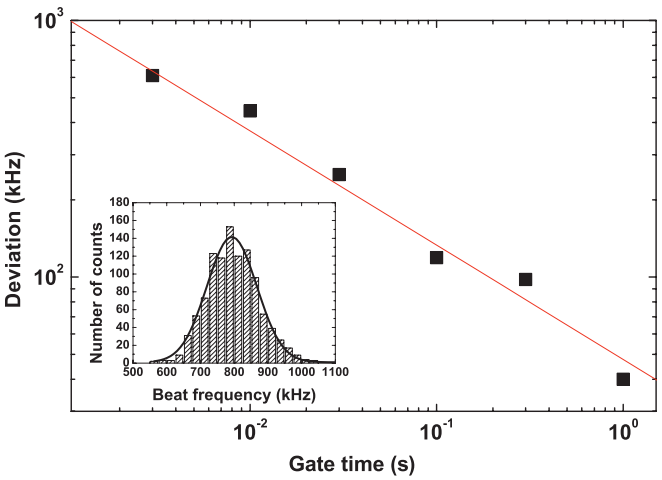

FIG. 6. (Color online) Allan deviation of the locked Ti:sapphire laser referenced to the OFC. The deviation is the widths of the beat-note frequency distribution measured with various integration times (1 ms to 1 s), while the laser is locked to the OFC. The inset is the frequency distribution fitted to a Gaussian profile with a 0.1 s integration time.

TABLE II. Absolute frequencies of atomic lithium $2^2S_{1/2} \rightarrow 3^2S_{1/2}$ transitions including two isotopes and two hyperfine components. C.G. denotes the center of gravity. The results of the previous experiments are also included for comparison.

Isotope		Frequency (MHz)	Ref.
^{7}Li	$F = 2$–2	815 617 949.98(12)	This work
	$F = 1$–1	815 618 567.23(14)	This work
	C. G.	815 618 181.45(9)	This work
		815 618 181.57(18)	[18]
		815 618 185.2(30)	[17]
	Theory	815 618 149.0(300)	[10]
		815 618 170.0(180)	[7]
^{6}Li	$F = 3/2$–3/2	815 606 668.99(22)	This work
	$F = 1/2$–1/2	815 606 844.40(33)	This work
	C. G.	815 606 727.46(18)	This work
		815 606 727.71(24)	[18]
		815 606 727.59(18)	[18]
		815 606 731.4(30)	[17]
	Isotope shift	−11 453.99(19)	This work
		−11 453.970(34)	[21]
		−11 453.85(19)	[18]
		−11 453.984(20)	[4]
		−11 453.95(13)	[20]
		−11 453.734(30)	[17]

III. RESULTS

The absolute frequencies of ^{6,7}Li $2S \rightarrow 3S$ hyperfine transitions and the derived isotope shift are listed in Table II, in comparison with previous experimental results. Our measurements are in very good agreement with the GSI experiment [18] with an accuracy improved by a factor of 2 for ^{7}Li. Both of these measurements are nearly 1 σ away from the theoretical predictions [7,10]. The earlier measurement using an interferometric method [17] in 2003 showed a clear discrepancy.

The experimental isotope shifts are briefed in the last section of Table II. Our result of −11 453.99(19) MHz shows good agreement with the reported isotope shift measurements. The experiment [17], which employed an interferometric method, shows a clear disagreement with all the others. The results of the previous optical frequency comb experiment [18], where the asymmetrical line shape is more pronounced, is slightly further away from ours in comparison to the direct rf beat-note frequency measurements [4,20,21].

The difference of the ^{6,7}Li charge radii can be calculated from the isotope shift using

$$\delta\langle r_c^2\rangle = \langle r_c^2(^7\mathrm{Li})\rangle - \langle r_c^2(^6\mathrm{Li})\rangle = \frac{\Delta\nu_{\mathrm{expt}} - \Delta\nu_{\mathrm{theor}}}{C_{2S-3S}},$$

where $\Delta\nu_{\mathrm{expt}}$ is the measured isotope shift of the $2S \rightarrow 3S$ transition, and the $\Delta\nu_{\mathrm{theor}}$ and C_{2S-3S} have been calculated to high precisions [21]. Hence, the difference of radii is $-0.74(12)\,\mathrm{fm}^2$, which is in a good agreement with the measurement of the electron scattering [26], $-0.79(25)\,\mathrm{fm}^2$. Meanwhile, with the precisely known ground state hyperfine splittings [27], the magnetic dipole hyperfine constants of the $3S$ state can be derived as 35.20 and 93.13 MHz for ^{6}Li and ^{7}Li, respectively.

IV. CONCLUSIONS

In summary, the absolute frequencies of ^{6,7}Li $2S \rightarrow 3S$ hyperfine transitions have been measured using a direct fluorescence detection scheme with a weakly collimated atomic beam to mitigate the asymmetry of the line shape and the ac Stark effect. These results yield the most accurate determination and offer an independent check of previous experiments utilizing the three-photon ionization technique. The statistical uncertainty of ^{6}Li can be improved by an isotope-enriched lithium source. The experiment can be further improved using an enhancement cavity to eliminate the error from the imperfect beam collinearity. Meanwhile, a better detection efficiency, including the reduction of background scattering and the improvement of the fluorescence collecting system, can also improve the S/N ratio while maintaining low intensity to avoid line shape asymmetry.

We acknowledge support from the National Science Council of Taiwan under Contracts No. NSC 97-2112-M-007-004-MY3 and No. NSC 96-2112-M-007-014-MY3.

[1] T. Zelevinsky, D. Farkas, and G. Gabrielse, Phys. Rev. Lett. **95**, 203001 (2005).
[2] R. Pohl *et al*., Nature (London) **466**, 213 (2010).
[3] L.-B. Wang *et al*., Phys. Rev. Lett. **93**, 142501 (2004).
[4] R. Sánchez *et al*., Phys. Rev. Lett. **96**, 033002 (2006).
[5] G. W. F. Drake and Z.-C. Yan, Can. J. Phys. **86**, 45 (2008).
[6] M. Puchalski and K. Pachucki, Hyperfine Interact. **196**, 35 (2010).
[7] M. Puchalski and K. Pachucki, Phys. Rev. A **78**, 052511 (2008).
[8] M. Puchalski, D. Kdziera, and K. Pachucki, Phys. Rev. A **80**, 032521 (2009).
[9] J. S. Sims and S. A. Hagstrom, Phys. Rev. A **80**, 052507 (2009).
[10] Z.-C. Yan, W. Nörtershäuser, and G. W. F. Drake, Phys. Rev. Lett. **100**, 243002 (2008).
[11] V. A. Yerokhin, Phys. Rev. A **78**, 012513 (2008).
[12] J. Walls, R. Ashby, J. J. Clarke, B. Lu, and W. A. van Wijngaarden, Eur. Phys. J. D **22**, 159 (2003).
[13] W. A. van Wijngaarden, Can. J. Phys. **83**, 327 (2005).
[14] G. A. Noble and W. A. van Wijngaarden, Can. J. Phys. **87**, 807 (2009).
[15] C. J. Sansonetti, C. E. Simien, J. D. Gillaspy, J. N. Tan, S. M. Brewer, R. C. Brown, S.-J. Wu, and J. V. Porto, Phys. Rev. Lett. **107**, 023001 (2011).
[16] W. DeGraffenreid and C. J. Sansonetti, Phys. Rev. A **67**, 012509 (2003).
[17] B. A. Bushaw, W. Nörtershäuser, G. Ewald, A. Dax, and G. W. F. Drake, Phys. Rev. Lett. **91**, 043004 (2003).
[18] R. Sánchez *et al*., New J. Phys. **11**, 073016 (2009).
[19] W. Nörtershäuser *et al*., Hyperfine Interact. **162**, 93 (2005).
[20] G. Ewald *et al*., Phys. Rev. Lett. **93**, 113002 (2004).
[21] W. Nörtershäuser *et al*., Phys. Rev. A **83**, 012516 (2011).
[22] C.-C. Liao, K.-Y. Wu, Y.-H. Lien, H. Knöckel, H.-C. Chui, E. Tiemann, and J.-T. Shy, J. Opt. Soc. Am. B **27**, 1208 (2010).
[23] W. N. Venables and B. D. Ripley, *Modern Applied Statistics with S*, 4th ed. (Springer, New York, 2002).
[24] W. R. Johnson, U. I. Safronova, A. Derevianko, and M. S. Safronova, Phys. Rev. A **77**, 022510 (2008); U. Volz and H. Schmoranzer, Phys. Scr. T **65**, 48 (1996).
[25] G. Grynberg and B. Cagnac, Rep. Prog. Phys. **40**, 791 (1977).
[26] C. W. de Jager, H. de Vries, and C. de Vries, At. Data Nucl. Data Tables **14**, 479 (1974).
[27] A. Beckmann, K. D. Böklen, and D. Elke, Z. Phys. A **270**, 173 (1974).